Integrative Molecular Medicine

Research Article ISSN: 2056-6360

An epigenome-wide association study based on cell type-specific whole-genome bisulfite sequencing: Screening for DNA methylation signatures associated with bone mass

Shohei Komaki[1], Hideki Ohmomo[1,2], Tsuyoshi Hachiya[1], Ryohei Furukawa[1], Yuh Shiwa[1,2], Mamoru Satoh[1,2], Ryujin Endo[3,4], Minoru Doita[5], Makoto Sasaki[6,7] and Atsushi Shimizu[1]

[1]Division of Biomedical Information Analysis, Iwate Tohoku Medical Megabank Organization, Disaster Reconstruction Center, Iwate Medical University, 2-1-1 Nishitokuta, Yahaba, Shiwa, Iwate 028-3694, Japan

[2]Division of Biobank and Data Management, Iwate Tohoku Medical Megabank Organization, Disaster Reconstruction Center, Iwate Medical University, 2-1-1 Nishitokuta, Yahaba, Shiwa, Iwate 028-3694, Japan

[3]Division of Public Relations and Planning, Iwate Tohoku Medical Megabank Organization, Disaster Reconstruction Center, Iwate Medical University, 2-1-1 Nishitokuta, Yahaba, Shiwa, Iwate 028-3694, Japan

[4]Division of Medical Fundamentals for Nursing, Iwate Medical University, 2-1-1 Nishitokuta, Yahaba, Shiwa, Iwate 028-3694, Japan

[5]Department of Orthopaedic Surgery, School of Medicine, Iwate Medical University, 19-1 Uchimaru, Morioka, Iwate 020-8505, Japan

[6]Iwate Tohoku Medical Megabank Organization, Disaster Reconstruction Center, Iwate Medical University, 2-1-1 Nishitokuta, Yahaba, Shiwa, Iwate 028-3694, Japan

[7]Division of Ultrahigh Field MRI, Institute for Biomedical Sciences, Iwate Medical University, 2-1-1 Nishitokuta, Yahaba, Shiwa, Iwate 028-3694, Japan

Abstract

Bone mass can change intra-individually due to aging or environmental factors. Understanding the regulation of bone metabolism by epigenetic factors, such as DNA methylation, is essential to further our understanding of bone biology and facilitate the prevention of osteoporosis. To date, a single epigenome-wide association study (EWAS) of bone density has been reported, and our knowledge of epigenetic mechanisms in bone biology is strictly limited. Here, we conducted an EWAS based on cell type-specific whole-genome bisulfite sequencing (WGBS) of $CD3^+/CD4^+$ T cells and $CD14^{++}/CD16^-$ monocytes collected from 102 Japanese individuals, and screened DNA methylation signatures associated with bone mass. Analyses based on each cell type revealed that distinct sets of DNA methylation signatures were associated with bone mass. Some genes annotated to those DNA methylation signatures have known cell type-specific roles in bone metabolism. The results of our comprehensive screening might also contain additional novel bone-related loci, which could further our understanding of the epigenetic mechanisms of bone metabolism. With few exceptions, the cell type-specific DNA methylation signatures identified in this study are not covered by widely used arrays. Our WGBS-based EWAS highlights the importance of cell type-specific analysis with broad genome coverage, especially for discovery phase.

Introduction

The skeletal system is the most important feature supporting physical activity in human beings. Bone fracture seriously limits basic activity, and decreased bone mass is one of the major risk factors for fracture. Thus, preventing decreases in bone mass is crucial for sustaining the daily life of humans. Genetic mechanisms of osteogenesis have been well studied, and to date, various genetic markers have been reported to be associated with bone mass and density through genome-wide association studies (GWASs) [1–3]. However, bone mass and density are decreased temporarily as a result of posteriori factors, including aging, calcium and vitamin D intake, body weight, and physical activity [4–8]. Therefore, an association study focusing on epigenetic features, such as DNA methylation, which can change according to lifestyle and/or aging, should provide new insights into posteriori epigenetic mechanisms affecting bone formation and homeostasis.

DNA methylation (DNAm) is a biochemical alteration of DNA that can modulate gene transcription. Unlike nucleotide sequences, DNAm patterns vary depending on environmental factors [9]. Therefore, through the analysis of DNAm patterns, we can infer the effect of environmental factors on gene expression and subsequent phenotypes.

To date, only a single epigenetic-wide association study (EWAS) on bone mineral density has been published. In the study, the authors used a bead array (HM450, Illumina Infinium HumanMethylation450 BeadArray) and identified a single DNAm signature associated with bone density [10]. In array-based experimental systems, the number of target CpG sites is limited and increases the likelihood of overlooking

Correspondence to: Atsushi Shimizu, Ph.D., Professor, Division of Biomedical Information Analysis, Iwate Tohoku Medical Megabank Organization, Disaster Reconstruction Center, Iwate Medical University 2-1-1 Nishitokuta, Yahaba, Shiwa, Iwate 028-3694, Japan, Tel: +81-19-651-5110, ext. 5473; E-mail: ashimizu@iwate-med.ac.jp

Key words: *bone mass, CD3+/CD4+ T cell, CD14++/CD16- monocyte, epigenome-wide association study, whole genome bisulfite sequence*

Received: October 05, 2017; **Accepted:** October 09, 2017; **Published:** October 12, 2017

potentially significant CpG sites. HM450, the most widely applied platform for human EWAS, includes approximately 480,000 probes, which cover only 1.7 % of the 28.0 million CpG sites that exist in the human genome (GRCh37) [11]. Illumina Infinium Methylation EPIC BeadChip, is a newly designed microarray-based platform, but still covers only 3.0 % of all human genome CpG sites [12]. Reduced-representation bisulfite sequencing (RRBS) covers 10% of CpG sites in the genome [13] and methyl-capture sequencing, for example SureSelect Human Methyl-Seq (Agilent Technologies), is designed to capture 4.8 million CpG sites within ± 200 kbp of target regions which cover 17.1% of all CpG sites in the genome [14]. Methylated-cytosine enrichment methods such as methylated DNA immunoprecipitation sequencing (MeDIP-Seq) and methylated DNA binding domain sequencing (MBD-Seq) can cover ~50% of all CpG sites in the human genome [13]. However, MeDIP-Seq and MBD-Seq measure the relative enrichment of methylated DNA, are less accurate for quantifying DNA methylation levels [15], and their DNAm quantifications lack single-nucleotide resolution [16]. Meanwhile, whole-genome bisulfite sequencing (WGBS) can cover ~95% of all CpG sites in the human genome with single-nucleotide resolution [17].

The bone mineral density EWAS performed by Morris *et al.* [10] used whole blood samples. However, they emphasized the need for a cell type-specific study because different blood cell types could have different roles in bone biology. For example, bone cell activities are regulated by cytokines derived from lymphocytes or macrophages that affect bone metabolism (osteoimmunological regulation) [18,19]. Furthermore, osteoclasts differentiate from monocytes, which means that monocytes have a direct relationship with bone cells [20,21]. Therefore, cell type-specific signatures associated with bone metabolism can be attenuated by analyzing the mixture of heterogeneous cells within whole blood samples.

Here, to increase our understanding of bone biology and the role of epigenetics in bone metabolism, we screened DNAm signatures associated with bone mass using WGBS-based EWAS in $CD3^+/CD4^+$ T cells and $CD14^{++}/CD16^-$ monocytes isolated from 102 Japanese participants.

Materials and methods

Subjects

In this study, 109 apparently healthy subjects were enrolled. The participants are part of the Tohoku Medical Megabank Community-Based Cohort Study (TMM CommCohort Study). Demographic characteristics of the study subjects are described in Table 1. All 109 subjects were residents of the Iwate Prefecture, Japan and recruited at the Yahaba Center in the Yahaba Town, Iwate Prefecture. Details of the recruitment process were previously reported [22]. All participants provided written informed consent, and the study was approved by the Ethics Committee of Iwate Medical University (Approval ID: HG H25-19).

Table 1. Description of the cohort studied

	CD4T	Monocytes
N (% Female)	102 (52.90)	102 (53.90)
Bone area ratio (%) (mean ± SD)	28.94 ± 4.59	28.99 ± 4.58
Age (year) (mean ± SD)	59.01 ± 11.30	59.50 ± 10.87
Number of CpG sites analyzed	24,036,660	23,940,752

From 109 subjects, 102 and 102 were used for the analyses of CD4T and monocytes, respectively, with 95 subjects overlapping. SD: standard deviation, CD4T: $CD3^+/CD4^+$ T cells.

Bone mass measurements

A dual-energy X-ray absorptiometry (DXA) is commonly used for bone mass measurements [23]. However, the TMM CommCohort Study employed quantitative ultrasonometry (QUS) of calcaneus using an ultrasound device, Benus evo ultrasound Bone Densitometer (Nihon Kohden Co., Tokyo, Japan) to evaluate the bone mass because the equipment is of transportable size and avoids the use of ionizing radiation. Benus measures the trabecular bone area ratio that is significantly and positively associated with bone mineral density as measured by the DXA method ($R^2 = 0.351$, $P < 0.001$) [24]. Therefore, in this study, the bone area ratio was used to represent bone mass. For 109 subjects, the trabecular bone mass was measured by an identical ultrasound device at the Yahaba Center following the manufacturer's instructions.

Sample preparation and DNA methylation profiling

Detailed methods for sample preparation and DNAm profiling were previously described by Hachiya *et al.* [25]. In brief, for the isolation of peripheral blood mononuclear cells, 8 ml of whole blood was collected from each participant, and $CD3^+/CD4^+$ T cells (CD4T) and $CD14^{++}/CD16^-$ monocytes were further isolated. Genomic DNA extracted from each cell type went through bisulfite conversion and library preparation, followed by WGBS. After removal of the adapter, sequence reads (length ≥ 20 bp) were mapped onto the GRCh37d5 reference genome. Overlaps between paired-end reads were clipped. Then, DNAm levels at each CpG site were estimated by dividing the number of the mapped reads that contained unconverted cytosine by the total number of mapped reads. CpG sites with extreme depth (< 6 or > 300) or with a high frequency of missing data among subjects (call rate < 50%) were excluded from the dataset.

Epigenome wide association analysis

We performed six epigenome-wide association analyses based on DNAm profiles of: (1) CD4T of all subjects, (2) CD4T of females, (3) CD4T of males, (4) monocytes of all subjects, (5) monocytes of females, and (6) monocytes of males. A linear regression (LM) model was used to test the relationship between the DNAm level of each ~24 million CpG sites and bone mass. CpG sites on sex chromosomes and mitochondrion were excluded from the analyses. The LM was performed using the lm function of the R version 3.2.0, specifying bone mass as the dependent variable and DNAm level, age, and BMI as the explanatory variables. Analyses (1) and (4) were further adjusted by sex. Each analysis was assessed based on the genomic inflation factor (λ) and quantile-quantile plot (QQ plot). In this study, a less stringent threshold of P value = 1.0×10^{-7}, suggested for the discovery criteria, was applied [26].

Results

Mean and standard deviation (SD) of bone mass (%) among all 109 subjects were 28.94 and 4.51, respectively (Table 1). Females showed lower bone mass mean value and larger sd than did males (Table 1) (F test P value = 0.032, Wilcoxon rank sum test P value = 0.009). The bone mass of females greatly fluctuates in association with estrogen level, especially at the early menopause stage [27,28], which can explain the observed gender differences in bone mass. These results imply that there are sex-specific mechanisms characterizing the bone mass of study subjects, and emphasize the need for sex-specific analyses to explore the epigenetic regulation of bone metabolism.

From the 109 subjects, DNAm profiles of CD4T and monocytes were obtained from 102 and 102 subjects, respectively (Table 1),

with 95 subjects overlapped. For CD4T, 24,036,660 CpG sites were analyzed, and 23,940,752 sites were analyzed for monocytes. Resultant *P* values of each analysis, based on different datasets, are presented as Manhattan and QQ plots (Figure 1 and Supplementary Figure S1). Genomic inflation factors for each analysis approximate to 1, indicating that confounding factors were well controlled in the analyses (Supplementary Figure S1).

CpG sites with *P* values below the threshold of 1.0×10^{-7} in each analysis are listed in Tables 2 and 3. In analyses based on CD4T of both sexes, females only, and males only, 18, 4, and 9 CpG sites showed *P* values $< 1.0 \times 10^{-7}$, respectively. Analyses based on monocytes of both sexes, females only, and males only identified 18, 22, and 7 CpG sites with *P* values $< 1.0 \times 10^{-7}$, respectively.

Discussion

We screened CpG signatures associated with bone mass by means of WGBS-based EWAS. As a result, different sets of CpG signatures were identified among cell type- and sex-specific analyses. Genes located close (within ± 1 Mbp) to CpG sites with *P* values $< 1.0 \times 10^{-7}$ are listed in Tables 2 and 3. Among them, *WWP2*, *BICC1*, and *MAPK14*, have known biological functions related to bone development or homeostasis. *WWP2* encodes a member of the NEDD4 family of E3 ligases that function in protein ubiquitylation. Indeed, monoubiquitylation of goosecoid by WWP2 protein in chondrocytes regulates craniofacial skeletal patterning [29]. Furthermore, knockdown and overexpression experiments of *Wwp2* in mesenchymal stem cells of mice by Zhu *et al.* [30] suggested that WWP2 behaves as positive regulator for osteogenesis through ubiquitylation of RUNX2, which is required for the early stage of osteoblast differentiation. Therefore, suppressed transcription of *WWP2* can be responsible for lowered bone mass, and might explain the negative association observed between bone mass and *WWP2* DNAm level in CD4T.

BICC1 is a gene encoding an RNA-binding protein. Knockdown experiments in mice and GWAS of human bone mineral density show that *Bicc1/BICC1* plays a significant role in osteoblastogenesis and affects bone mineral density [31]. Briefly, BICC1 positively regulates osteoblastogenesis, and suppression of *BICC1* expression leads to decreased bone mineral density. In both mice and humans, the association between *Bicc1*/*BICC1* and bone mineral density was demonstrated in male subjects. Consistently, a significant association was observed between *BICC1* DNAm and bone mass in monocytes of male subjects in this study. The negative association between DNAm level of the CpG on *BICC1* and bone mass implies that methylation of the site decreases *BICC1* expression, leading to lowered bone mass in male subjects. Of all blood cell types, only plasma and monocyte show expression of BICC1 (GeneCards database, http://www.genecards.org; accessed on July 1, 2017), which could explain why a *BICC1* DNAm signature was identified from monocytes but not from CD4T cells in this study.

Mitogen-activated protein kinase 14 (p38α), encoded by *MAPK14*, has a function in bone resorbing. Expression of genes essential for osteoclast differentiation, such as *SP7*, *ALPL*, and *BGLAP*, is regulated by p38α [32]. Using a specific p38α kinase inhibitor, osteoclast differentiation is suppressed. Furthermore, it is suggested that phosphorylation of microphthalmia-associated transcription factor, required for the osteoclast maturation, is stimulated by phosphorylated

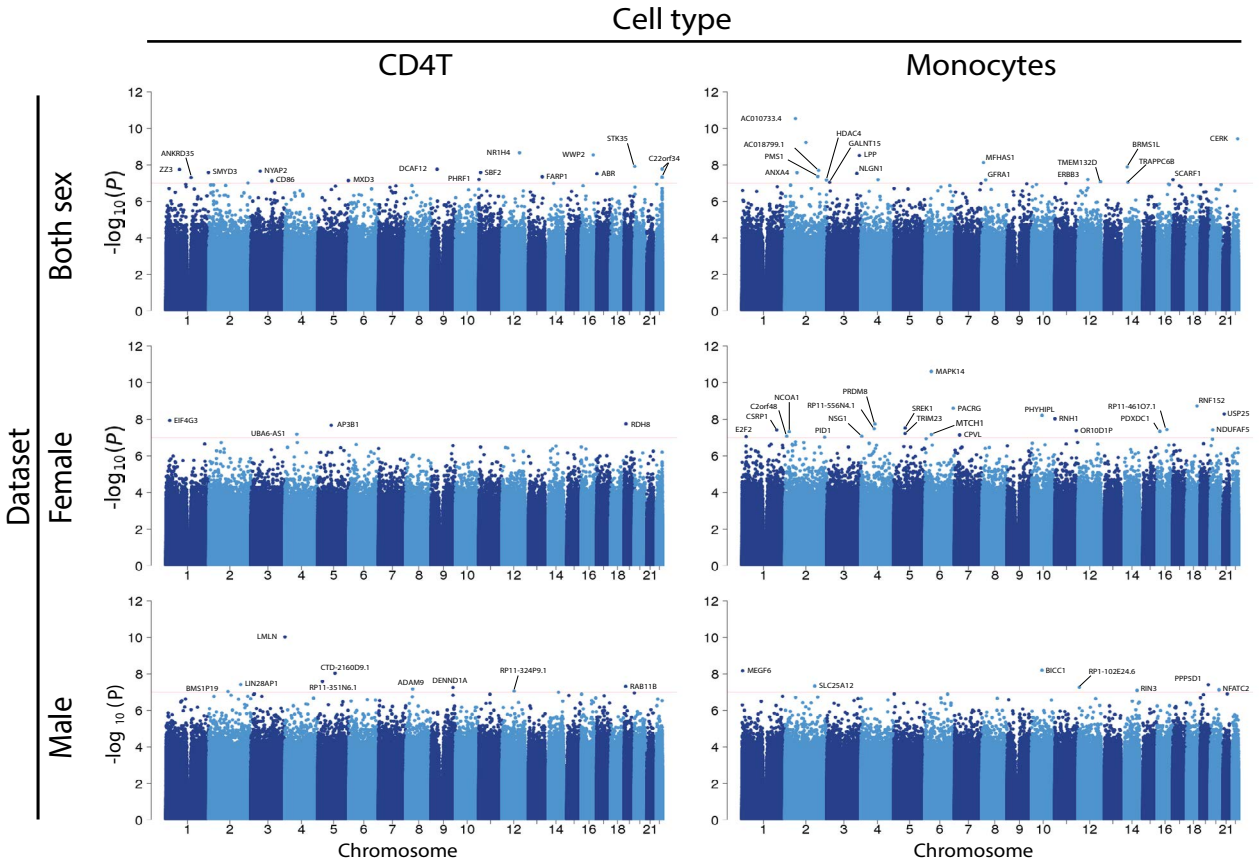

Figure 1. Manhattan plots for each association analysis based on different cell types and datasets. The red line indicates *P* value = 1.0×10^{-7}. CD4T: $CD3^+/CD4^+$ T cells.

p38α [33]. Since osteoclasts function in bone resorption, stimulated osteoclast formation can lead to excess bone loss. The function of p38α to negatively affect osteogenesis through activating osteoclastogenesis and osteoclast function might explain the negative association between bone mass and CpG DNAm levels of *MAPK14*. This association was observed only from the analysis based on monocytes of females. This is consistent with the facts that osteoclasts are derived from monocytes [20,21], and that the p38α pathway is an important regulator of osteoporosis in postmenopausal women and induced by estrogen deficiency [28].

Other genes listed in Table 2 are thought to function in bone metabolism, or are associated with bone density through GWAS (*ERBB3*, [34]; *SBF2*, [35]; *RNH1*, [36]; *NFATC2*, [37]; *RIN3*, [38]; *ADAM9*, [39]; *HDAC4*, [40]; and *CD86*, [41]).

Furthermore, genes other than above mentioned may have unreported functions in bone metabolism including osteogenesis and osteoclastogenesis. For example, *NR1H4*, also known as farnesoid X receptor alpha (*FXRα*), is a member of the nuclear receptor superfamily of ligand-dependent transcription factors. A CpG site, chr12:100925094, whose DNAm level is significantly associated with bone mass, is located on *NR1H4*. This receptor is an activator of gluconeogenic pathways and a known regulator of glucocorticoid receptor expression and activity [42]. Glucocorticoids have a detrimental effect on bone formation and homeostasis through suppressing the differentiation and replication of osteoblast cells, and by inhibiting the function of mature osteoblast cells [43]. In addition, increased osteoblast apoptosis is induced by glucocorticoids and glucocorticoids decrease the function of osteocytes [43]. Given their anti-inflammatory and immunosuppressive properties, glucocorticoids have been widely used as therapeutic agents, even though glucocorticoid therapy can cause bone loss and fractures in patients. The negative correlation between bone mass and DNAm level of *NR1H4* CpG observed in this study implies that DNAm suppresses the transcription or function of *NR1H4*, resulting in bone loss.

A previous EWAS of bone mineral density reported eight CpG sites as suggestive DNAm signatures in individual cohorts but did not identify any DNAm signatures common across the studied cohorts [10]. In this study, these eight previously reported CpG sites showed no significant associations with bone mass (*P* values of > 0.130) (Supplementary Table S1). However, we analyzed Japanese individuals applying bone area ratio of calcaneus measured by QUS as bone mass, and DNAm level was measured using purified CD4T and monocyte cells. The different materials and methods used in the two studies might have been the cause for the differing results. Thus, our results do not deny possible relationships between bone mineral density and DNAm levels of the CpG sites suggested by Morris *et al.* [10].

Table 2. CpG sites associated with bone mass ($P < 1.0 \times 10^{-7}$) identified in $CD3^+/CD4^+$ T cells

Dataset	Position[*1]	DNAm level (mean ± SD)	Coefficient (95% CI)	*P* value	Gene
Both sexes	12:100925094	75.80 ± 29.19	-3.90 (-5.07 – -2.73)	2.15×10^{-9}	*NR1H4*
	16:69898597	97.71 ± 5.11	-0.71 (-0.93 – -0.50)	2.85×10^{-9}	*WWP2*[*2]
	20:2119971	97.59 ± 2.92	-0.38 (-0.50 – -0.26)	1.22×10^{-8}	*STK35*
	22:49949200	95.19 ± 5.08	-0.64 (-0.85 – -0.43)	1.69×10^{-8}	RP1-29C18.10/*C22orf34*
	9:34115355	94.55 ± 6.92	-0.89 (-1.17 – -0.60)	1.73×10^{-8}	*DCAF12*
	1:78131263	98.89 ± 3.26	-0.46 (-0.61 – -0.32)	1.79×10^{-8}	*ZZZ3*
	3:54141925	97.46 ± 7.70	-1.14 (-1.50 – -0.79)	2.21×10^{-8}	
	11:10061108	97.46 ± 4.62	-0.56 (-0.74 – -0.38)	2.61×10^{-8}	*SBF2*[*3]
	1:246227233	97.04 ± 3.09	-0.39 (-0.52 – -0.27)	2.62×10^{-8}	*SMYD3*
	17:980028	98.17 ± 2.88	-0.36 (-0.48 – -0.24)	3.09×10^{-8}	*ABR*
	13:98739376	92.83 ± 9.98	-1.22 (-1.63 – -0.81)	4.52×10^{-8}	*FARP1*
	22:49831298	92.28 ± 4.83	-0.60 (-0.80 – -0.40)	4.74×10^{-8}	*C22orf34*
	22:49967265	93.68 ± 6.72	-0.83 (-1.11 – -0.55)	4.90×10^{-8}	RP1-29C18.9/*C22orf34*
	1:145549040	1.07 ± 2.81	0.35 (0.23 – 0.46)	4.99×10^{-8}	*ANKRD35*
	11:609352	96.70 ± 6.47	-0.80 (-1.07 – -0.53)	6.28×10^{-8}	*PHRF1*
	5:176738773	0.47 ± 1.07	0.13 (0.09 – 0.18)	7.26×10^{-8}	*MXD3*
	3:121842023	96.57 ± 3.27	-0.40 (-0.54 – -0.27)	7.56×10^{-8}	*CD86*[*3]
	2:226290206	95.65 ± 6.08	-0.75 (-1.01 – -0.49)	9.82×10^{-8}	*NYAP2*
Female	1:21478594	95.61 ± 7.46	-1.38 (-1.78 – -0.98)	1.18×10^{-8}	*EIF4G3*
	19:10127122	98.74 ± 2.59	-0.46 (-0.60 – -0.32)	1.80×10^{-8}	*RDH8*
	5:77319949	98.40 ± 4.02	-0.68 (-0.89 – -0.48)	2.15×10^{-8}	*AP3B1*
	4:68576716	99.05 ± 2.77	-0.49 (-0.64 – -0.33)	6.60×10^{-8}	*UBA6-AS1*
Male	3:197772225	96.91 ± 3.43	-0.70 (-0.86 – -0.53)	9.36×10^{-11}	*LMLN*
	5:99290935	96.48 ± 2.76	-0.50 (-0.64 – -0.35)	9.22×10^{-9}	*CTD-2160D9.1*
	5:26240956	97.78 ± 3.46	-0.63 (-0.82 – -0.44)	2.59×10^{-8}	RP11-351N6.1
	2:184159598	95.89 ± 3.58	-0.65 (-0.84 – -0.45)	3.80×10^{-8}	*LIN28AP1*
	19:8455454	0.61 ± 1.52	0.27 (0.19 – 0.36)	4.92×10^{-8}	*RAB11B*/RAB11B-AS1
	9:126673994	96.62 ± 5.29	-0.99 (-1.29 – -0.68)	5.63×10^{-8}	*DENND1A*
	8:38854608	0.45 ± 1.40	0.25 (0.17 – 0.33)	6.76×10^{-8}	*ADAM9*[*3]
	12:69611102	94.12 ± 5.56	-0.98 (-1.29 – -0.67)	8.77×10^{-8}	RP11-324P9.1
	2:110449774	84.72 ± 9.25	-1.66 (-2.19 – -1.13)	9.34×10^{-8}	*BMS1P19*

[*1] Chromosome number and position of the CpG site.
[*2] Gene with evident roles in bone development and/or homeostasis.
[*3] Gene with a suggested function in, or relationship with, bone development and/or homeostasis.
DNAm: DNA methylation, SD: standard deviation, CI: confidence interval.

We note that the number of subjects enrolled in this study was around 100, and trabecular bone area ratio of calcaneus measured by QUS was applied as a phenotypic variable. Therefore, our study was based on limited data. Furthermore, the association analyses were performed based on a single Japanese cohort and associations between DNAm levels and bone mass were not validated in any other independent cohorts. Therefore, associations reported in this study remain to be confirmed by additional studies.

Despite the above-mentioned limitations, whole-genome DNAm analyses applied in this study might provide new insights into the role of DNAm in bone metabolism. Among 78 DNAm signatures identified in the present EWAS, only a single CpG site [chr16:15188395 (cg16603896); Table 3] is a target of the most commonly applied platform for DNA methylation studies in humans, HM450. In this study, furthermore, several CpG sites were identified as DNAm signatures with small *P* values, while neighboring CpG sites surrounding the

Table 3. CpG sites associated with bone mass ($P < 1.0 \times 10^{-7}$) identified in monocytes

Dataset	Position[*1]	DNAm level (mean ± SD)	Coefficient (95% CI)	*P* value	Gene
Both sexes	2:61108446	0.29 ± 1.38	0.21 (0.15 – 0.26)	2.91×10^{-11}	AC010733.4
	22:47133916	0.84 ± 2.80	0.40 (0.28 – 0.51)	3.73×10^{-10}	*CERK*
	2:121815071	96.54 ± 4.01	-0.56 (-0.72 – -0.39)	5.95×10^{-10}	Y RNA
	3:188489102	98.19 ± 3.52	-0.46 (-0.60 – -0.32)	3.02×10^{-9}	*LPP*
	8:8750676	1.11 ± 1.71	0.22 (0.15 – 0.30)	7.51×10^{-9}	*MFHAS1*
	14:36295936	0.51 ± 1.43	0.19 (0.13 – 0.25)	1.30×10^{-8}	RP11-317N8.5/*BRMS1L*
	2:195259677	85.29 ± 14.8	-2.22 (-2.89 – -1.55)	2.02×10^{-8}	AC018799.1
	2:69941555	97.83 ± 3.04	-0.39 (-0.52 – -0.26)	2.66×10^{-8}	*ANXA4*
	3:173900045	85.08 ± 18.96	-2.76 (-3.64 – -1.89)	2.95×10^{-8}	*NLGN1*
	2:190657692	96.39 ± 3.84	-0.48 (-0.64 – -0.32)	4.33×10^{-8}	*PMS1*
	12:56474020	0.25 ± 1.11	0.14 (0.09 – 0.18)	6.30×10^{-8}	*ERBB3*[*3]
	17:1535968	92.9 ± 13.44	-1.63 (-2.19 – -1.08)	6.43×10^{-8}	*SCARF1*
	4:99080231	92.82 ± 9.63	-1.41 (-1.86 – -0.95)	6.45×10^{-8}	Y RNA
	8:21530651	94.44 ± 12.01	-1.60 (-2.13 – -1.07)	6.62×10^{-8}	*GFRA2*
	2:240322590	0.50 ± 1.79	0.22 (0.15 – 0.30)	6.72×10^{-8}	*HDAC4*[*3]
	12:129772248	90.49 ± 7.00	-0.85 (-1.14 – -0.56)	8.41×10^{-8}	*TMEM132D*
	3:16191417	96.63 ± 7.87	-1.00 (-1.34 – -0.66)	9.09×10^{-8}	*GALNT15*
	14:39639583	1.60 ± 2.61	0.32 (0.21 – 0.43)	9.11×10^{-8}	*TRAPPC6B*
Female	6:35995637	0.37 ± 1.07	0.21 (0.16 – 0.25)	2.44×10^{-11}	*MAPK14*[*2]
	18:59560980	0.51 ± 1.48	0.27 (0.20 – 0.35)	1.87×10^{-9}	*RNF152*
	6:163371471	94.89 ± 8.66	-2.42 (-2.96 – -1.87)	2.54×10^{-9}	*PACRG*
	21:17220599	97.23 ± 4.77	-0.89 (-1.14 – -0.63)	5.16×10^{-9}	*USP25*
	10:60936039	6.68 ± 5.35	0.98 (0.70 – 1.26)	6.22×10^{-9}	*PHYHIPL*
	11:497792	96.88 ± 4.27	-0.78 (-1.01 – -0.56)	9.53×10^{-9}	*RNH1*[*3]
	4:81105396	0.52 ± 1.96	0.35 (0.25 – 0.45)	1.84×10^{-8}	RP11-377G16.2/*PRDM8*
	5:65423122	84.35 ± 21.30	-3.75 (-4.89 – -2.60)	3.07×10^{-8}	*SREK1*
	4:76766071	97.61 ± 3.13	-0.55 (-0.72 – -0.38)	3.34×10^{-8}	RP11-556N4.1
	16:56225078	0.77 ± 2.84	0.50 (0.36 – 0.65)	3.68×10^{-8}	RP11-461O7.1
	20:13765582	0.34 ± 1.48	0.26 (0.18 – 0.34)	3.78×10^{-8}	*NDUFAF5*
	1:201449877	0.23 ± 0.96	0.17 (0.12 – 0.22)	3.86×10^{-8}	*CSRP1*
	11:124035292	98.58 ± 3.03	-0.53 (-0.70 – -0.37)	4.21×10^{-8}	*OR10D1P*
	16:15188395 (cg16603896)	0.96 ± 3.22	0.54 (0.37 – 0.71)	4.60×10^{-8}	RP11-72I8.1/*PDXDC1*
	2:24660027	92.65 ± 8.78	-1.53 (-2.00 – -1.06)	4.83×10^{-8}	*NCOA1*
	5:64919917	0.23 ± 0.96	0.16 (0.11 – 0.21)	6.02×10^{-8}	*TRIM23*
	6:36954391	0.47 ± 1.62	0.29 (0.20 – 0.39)	6.79×10^{-8}	*MTCH1*
	7:29157080	98.58 ± 3.53	-0.61 (-0.81 – -0.42)	7.31×10^{-8}	*CPVL*
	2:10338969	97.26 ± 3.76	-0.64 (-0.85 – -0.44)	8.54×10^{-8}	*C2orf48*
	4:4377945	95.56 ± 3.49	-0.61 (-0.80 – -0.41)	8.58×10^{-8}	*NSG1*
	1:23857808	0.97 ± 3.41	0.72 (0.50 – 0.93)	9.08×10^{-8}	*E2F2*
	2:230125683	84.64 ± 9.88	-1.72 (-2.27 – -1.17)	9.61×10^{-8}	*PID1*
Male	10:60540166	87.39 ± 10.86	-2.06 (-2.64 – -1.48)	6.42×10^{-9}	*BICC1*[*2]
	1:3463645	93.37 ± 4.07	-0.75 (-0.96 – -0.54)	6.84×10^{-9}	*MEGF6*
	19:47039387	98.04 ± 4.18	-0.84 (-1.08 – -0.59)	3.90×10^{-8}	*PPP5D1*
	2:172721808	91.63 ± 11.99	-2.36 (-3.07 – -1.65)	4.68×10^{-8}	*SLC25A12*
	12:6588863	96.45 ± 3.77	-0.66 (-0.86 – -0.46)	5.54×10^{-8}	*RP1-102E24.6*
	20:50007014	96.99 ± 4.16	-0.73 (-0.96 – -0.50)	7.50×10^{-8}	*NFATC2*[*3]
	14:93054727	92.29 ± 19.21	-3.50 (-4.60 – -2.40)	8.00×10^{-8}	*RIN3*[*3]

[*1] Chromosome number and the position of CpG site.
[*2] Gene with evident roles in bone development and/or homeostasis.
[*3] Gene with suggested function in, or relationship with, bone development and/or homeostasis.
DNAm: DNA methylation, SD: standard deviat

signatures did not show such associations between DNAm level and bone mass (Supplementary Figure S2). This result implies that, without the high genome-coverage, DNAm association studies could have overlooked a large number of potential DNAm signals. Therefore, this study emphasizes the importance of WGBS-based analysis with the highest genome-coverage, especially for discovery phrase requiring comprehensive screening with few genomic region omissions.

The aim of this study was to screen DNA methylation signatures associated with bone mass using cell type-specific analyses with the widest genome coverage. We have successfully conducted analyses and have presented candidate DNAm signatures. EWAS with larger-scale cohorts focusing on the specific regions identified in this study will further elucidate the role of epigenetic mechanisms in bone biology.

Acknowledgements

The authors appreciate the participants of the Tohoku Medical Megabank Project. We would like to thank the members of the Iwate Tohoku Medical Megabank Organization of Iwate Medical University (IMM) and the Tohoku Medical Megabank Organization of Tohoku University (ToMMo) for their encouragement and support. We deeply thank Ms. Kanako Ono for her assistance with sample processing and handling.

Funding information

- The Reconstruction Agency, the Ministry of Education, Culture, Sports, Science and Technology (MEXT)
- The Japan Agency for Medical Research and Development (AMED)

Competing interest

None

References

1. Cho YS, Go MJ, Kim YJ, Heo JY, Oh JH, et al. (2009) A large-scale genome-wide association study of Asian populations uncovers genetic factors influencing eight quantitative traits. *Nat Genet* 41: 527–534. [Crossref]
2. Rivadeneira F, Styrkársdottir U, Estrada K, Halldórsson BV, Hsu YH, et al. (2009) Twenty bone-mineral-density loci identified by large-scale meta-analysis of genome-wide association studies. *Nat Genet* 41: 1199–1206. [Crossref]
3. Estrada K, Styrkarsdottir U, Evangelou E, Hsu YH, Duncan EL, et al. (2012) Genome-wide meta-analysis identifies 56 bone mineral density loci and reveals 14 loci associated with risk of fracture. *Nat Genet* 44: 491-501. [Crossref]
4. Demontiero O, Vidal C, Duque G (2012) Aging and bone loss: new insights for the clinician. *Ther Adv Musculoskelet Dis* 4: 61-76. [Crossref]
5. Dawson-Hughes B, Harris SS, Krall EA, Dallal GE (1997) Effect of calcium and vitamin D supplementation on bone density in men and women 65 years of age or older. *N Engl J Med* 337: 670-676. [Crossref]
6. Booth SL, Broe KE, Gagnon DR, Tucker KL, Hannan MT, et al. (2003) Vitamin K intake and bone mineral density in women and men. *Am J Clin Nutr* 77: 512-516. [Crossref]
7. Shapses SA, Riedt CS (2006) Bone, body weight, and weight reduction: what are the concerns? *J Nutr* 136: 1453-1456. [Crossref]
8. Warden SJ, Mantila Roosa SM, Kersh ME, Hurd AL, Fleisig GS, et al. (2014) Physical activity when young provides lifelong benefits to cortical bone size and strength in men. *Proc Natl Acad Sci U S A* 111: 5337–5342.
9. Foley DL, Craig JM, Morley R, Olsson CA, Dwyer T, et al. (2009) Prospects for epigenetic epidemiology. *Am J Epidemiol* 169: 389-400. [Crossref]
10. Morris JA, Tsai PC, Joehanes R, ,Zheng J, Trajanoska K, et al. (2017) Epigenome-wide Association of DNA Methylation in Whole Blood With Bone Mineral Density. *J Bone Miner Res* 32: 1644-1650. [Crossref]
11. Bibikova M, Barnes B, Tsan C, Ho V, Klotzle B, et al. (2011) High density DNA methylation array with single CpG site resolution. *Genomics* 98: 288-295. [Crossref]
12. Pidsley R, Zotenko E, Peters TJ, Lawrence MG, Risbridger GP, et al. (2016) Critical evaluation of the Illumina MethylationEPIC BeadChip microarray for whole-genome DNA methylation profiling. *Genome Biol* 17: 208. [Crossref]
13. Walker DL, Bhagwate AV, Baheti S, Smalley RL, Hilker CA, et al. (2015) DNA methylation profiling: comparison of genome-wide sequencing methods and the Infinium Human Methylation 450 Bead Chip. *Epigenomics* 7: 1–16. [Crossref]
14. Teh AL, Pan H, Lin X, Lim YI, Patro CPK, et al. (2016) Comparison of Methyl-capture Sequencing vs. Infinium 450K methylation array for methylome analysis in clinical samples. *Epigenetics* 11: 36–48. [Crossref]
15. Bock C, Halbritter F, Carmona FJ, Tierling S, Datlinger P, et al. (2016) Quantitative comparison of DNA methylation assays for biomarker development and clinical applications. *Nat Biotechnol* 34: 726–737. [Crossref]
16. Harris RA, Wang T, Coarfa C, Nagarajan RP, Hong C, et al. (2010) Comparison of sequencing-based methods to profile DNA methylation and identification of monoallelic epigenetic modifications. *Nat Biotechnol* 28: 1097–1105.[Crossref]
17. Stirzaker C, Taberlay PC, Statham AL, Clark SJ (2014) Mining cancer methylomes: prospects and challenges. *Trends Genet* 30: 75-84. [Crossref]
18. Walsh MC, Kim N, Kadono Y, Rho J, Lee SY, et al. (2006) Osteoimmunology: Interplay between the immune system and bone metabolism. *Annu Rev Immunol* 24: 33–63. [Crossref]
19. Mori G, D'Amelio P, Faccio R, Brunetti G (2013) The Interplay between the bone and the immune system. *Clin Dev Immunol* 2013: 720504. [Crossref]
20. Udagawa N, Takahashi N, Akatsu T, Tanaka H, Sasaki T, et al. (1990) Origin of osteoclasts: mature monocytes and macrophages are capable of differentiating into osteoclasts under a suitable microenvironment prepared by bone marrow-derived stromal cells. *Proc Natl Acad Sci U S A* 87: 7260–7264. [Crossref]
21. Boyle WJ, Simonet WS, Lacey DL (2003) Osteoclast differentiation and activation. *Nature* 423: 337-342. [Crossref]
22. Kuriyama S, Yaegashi N, Nagami F, Arai T, Kawaguchi Y, et al. (2016) The Tohoku Medical Megabank Project: Design and Mission. *J Epidemiol* 26: 493-511. [Crossref]
23. Pisani P, Renna MD, Conversano F, Casciaro E, Muratore M, et al. (2013) Screening and early diagnosis of osteoporosis through X-ray and ultrasound based techniques. *World J Radiol* 5: 398–410.
24. Tatebe T, Takanashi Y, Mizutani Y, Miura T (1998) A study for validity of ultrasound bone densitometry using "Benus." *Res J Heal Sport Sci Chukyo Univ* 40: 103–110.
25. Hachiya T, Furukawa R, Shiwa Y, Ohmomo H, Ono K, et al. (2017) Genome-wide identification of inter-individually variable DNA methylation sites improves the efficacy of epigenetic association studies. *npj Genomic Med* 2: 11.
26. Panagiotou OA, Ioannidis JPA, Hirschhorn JN, Abecasis GR, Frayling TM, et al. (2012) What should the genome-wide significance threshold be? Empirical replication of borderline genetic associations. *Int J Epidemiol* 41: 273–286.
27. Clarke BL, Khosla S (2009) Androgens and bone. *Steroids* 74: 296-305. [Crossref]
28. Caverzasio J, Higgins L, Ammann P (2008) Prevention of trabecular bone loss induced by estrogen deficiency by a selective p38alpha inhibitor. *J Bone Miner Res* 23: 1389-1397. [Crossref]
29. Zou W, Chen X, Shim J, Huang Z, Brady N, et al. (2011) The E3 ubiquitin ligase Wwp2 regulates craniofacial development through mono-ubiquitylation of Goosecoid. *Nat Cell Biol* 13: 59–65. [Crossref]
30. Zhu W, He X, Hua Y, Li Q, Wang J, et al. (2017) The E3 Uubiquitin ligase WWP2 facilitates RUNX2 transactivation through a mono-ubiquitination manner during osteogenic differentiation. *J Biol Chem* 292: 11178–11188. [Crossref]
31. Mesner LD, Ray B, Hsu YH, Manichaikul A, Lum E, et al. (2014) Bicc1 is a genetic determinant of osteoblastogenesis and bone mineral density. *J Clin Invest* 124: 2736-2749. [Crossref]
32. Thouverey C, Caverzasio J (2015) Focus on the p38 MAPK signaling pathway in bone development and maintenance. *Bonekey Rep* 4: 711. [Crossref]
33. Mansky KC, Sankar U, Han J, Ostrowski MC (2002) Microphthalmia transcription factor is a target of the p38 MAPK pathway in response to receptor activator of NF-kappa B ligand signaling. *J Biol Chem* 277: 11077–10083. [Crossref]
34. Lin SH, Cheng CJ, Lee YC, Ye X, Tsai WW, et al. (2008) A 45-kDa ErbB3 secreted by prostate cancer cells promotes bone formation. *Oncogene* 27: 5195-5203. [Crossref]
35. Lei SF, Tan LJ, Liu XG, Wang L, Yan H, et al. (2009) Genome-wide association study identifies two novel loci containing FLNB and SBF2 genes underlying stature variation. *Hum Mol Genet* 18: 1661–1669. [Crossref]

36. Kantawong F, Burchmore R, Gadegaard N, Oreffo ROC, Dalby MJ (2009) Proteomic analysis of human osteoprogenitor response to disordered nanotopography. *J R Soc Interface* 6: 1075–1086. [Crossref]

37. Sitara D, Aliprantis AO (2010) Transcriptional regulation of bone and joint remodeling by NFAT. *Immunol Rev* 233: 286-300. [Crossref]

38. Kemp JP, Medina-Gomez C, Estrada K, St Pourcain B, Heppe DHM, et al. (2014) Phenotypic dissection of bone mineral density reveals skeletal site specificity and facilitates the identification of novel loci in the genetic regulation of bone mass attainment. *PLoS Genet* 10: e1004423. [Crossref]

39. Karadag A, Zhou M, Croucher PI (2006) ADAM-9 (MDC-9/meltrin-γ), a member of the a disintegrin and metalloproteinase family, regulates myeloma-cell-induced interleukin-6 production in osteoblasts by direct interaction with the avß5 integrin. Blood 107: 3271–3278. [Crossref]

40. Vega RB, Matsuda K, Oh J, Barbosa AC, Yang X, et al. (2004) Histone deacetylase 4 controls chondrocyte hypertrophy during skeletogenesis. *Cell* 119: 555–566. [Crossref]

41. Bozec A, Zaiss MM, Kagwiria R, Voll R, Rauh M, et al. (2014) T cell costimulation molecules CD80/86 inhibit osteoclast differentiation by inducing the IDO/tryptophan pathway. *Sci Transl Med* 6: 235–246. [Crossref]

42. Renga B, Mencarelli A, D'Amore C, Cipriani S, Baldelli F, et al. (2012) Glucocorticoid receptor mediates the gluconeogenic activity of the farnesoid X receptor in the fasting condition. *FASEB J* 26: 3021–3031. [Crossref]

43. Canalis E, Mazziotti G, Giustina A, Bilezikian JP (2007) Glucocorticoid-induced osteoporosis: pathophysiology and therapy. *Osteoporos Int* 18: 1319–28. [Crossref]

44. Weisenberger DJ (2014) Characterizing DNA methylation alterations from The Cancer Genome Atlas. *J Clin Invest* 124: 17-23. [Crossref]